Geochimica et Cosmochimica Acta, Vol. 68, No. 24, pp. 5113–5126, 2004

0016-7037/04 $30.00 + .00

doi:10.1016/j.gca.2004.07.021

Solubility and solution mechanism of H_2O in alkali silicate melts and glasses at high pressure and temperature

Bjorn O. Mysen* and George D. Cody
Geophyiscal Laboratory, 5251 Broad Branch Road NW, Washington, DC 20015, USA

(*Received December* 4, 2003; *accepted in revised form July* 14, 2004)

Abstract—The solubility behavior of H_2O in melts in the system Na_2O-SiO_2-H_2O was determined by locating the univariant phase boundary, melt = melt + vapor in the 0.8–2 GPa and 1000°–1300°C pressure and temperature range, respectively. The NBO/Si-range of the melts (0.25–1) was chosen to cover that of most natural magmatic liquids. The H_2O solubility in melts in the system Na_2O-SiO_2-H_2O (X_{H2O}) ranges between 18 and 45 mol% (O = 1) with $(\partial X_{H2O}/\partial P)_T \sim 14–18$ mol% H_2O/GPa. The $(\partial X_{H2O}/\partial P)_T$ is negatively correlated with NBO/Si (= Na/Si) of the melt. The $(\partial X_{H2O}/\partial T)_P$ is in the −0.03 to +0.05 mol% H_2O/°C range, and is negatively correlated with NBO/Si. The $[\partial X_{H2O}/\partial (NBO/Si)]_{P,T}$ is in the −3 to −8 mol% H_2O/(NBO/Si) range. Melts with NBO/Si similar to basaltic liquids (~0.6-~1.0) show $(\partial X_{H2O}/\partial T)_P < 0$, whereas more polymerized melts exhibit $(\partial X_{H2O}/\partial T)_P > 0$. Complete miscibility between hydrous melt and aqueous fluid occurs in the 0.8–2 GPa pressure range for melts with NBO/Si ≤0.5 at T >1100°C. Miscibility occurs at lower pressure the more polymerized the melt. *Copyright © 2004 Elsevier Ltd*

1. INTRODUCTION

The dynamics of magma aggregation at depth, magma ascent, emplacement, and eruption depend on the water content of the magmatic liquid because most magma properties governing these processes are affected by H_2O dissolved in the magmatic liquids (silicate melts). For example, dissolution of H_2O in melts at high pressure causes reduction of silica activity, which is reflected in the compositional trends during melting and crystallization of hydrous systems (e.g., Kushiro, 1972, 1990; Mysen and Boettcher, 1975; Gaetani et al., 1993). Furthermore, viscosity and values of other transport properties of hydrous melts are significantly different from those of the anhydrous equivalents (Kushiro, 1978; Watson, 1994; Schulze et al., 1996; Dingwell et al., 1998; Holtz et al., 1999; Romano et al., 2001). The density of hydrous magma is lower than that of anhydrous melts (e.g., Kushiro, 1978; Lange, 1994; Richet and Polian, 1998; Mysen and Wheeler, 2000a).

There is a substantial amount of data on H_2O-solubility and H_2O-solubility mechanisms in magmatic liquids in the pressure regime of the Earth's crust (see, for example, Goranson, 1936; Hamilton et al., 1964; Hamilton and Oxtoby, 1986; McMillan et al., 1986; Dixon and Stolper, 1995; Holtz et al., 1995, 1996; Nowak and Behrens, 1995; Shen and Keppler, 1995; Carroll and Blank, 1997; Dingwell et al., 1997; Behrens et al., 2001). Many igneous processes do, however, occur at higher pressures corresponding to those of the upper mantle. Data on water solubility and solubility mechanisms in silicate melts in that pressure and temperature regime are less common.

Available data on solubility mechanisms of water in silicate melts for the most part are limited to relationships between temperature, pressure and melt composition on the OH/H_2O(molecular) ratio, and most of these data have been obtained in the pressure and temperature regime of the Earth's crust (Stolper, 1982; Kohn et al., 1989, 1992; Silver and Stolper, 1985, 1989; Mysen and Virgo, 1986; Mysen, 1992; Nowak and Behrens, 1995; Shen and Keppler, 1995; Zhang et al., 1995; Sowerby and Keppler, 1999; Withers et al., 1999; Zhang, 1999; Schmidt et al., 2000, 2001a,b; Oglesby and Stebbins, 2000). An understanding of how the OH-groups are bonded to the silicate network is, however, important for characterization of the influence of dissolved water on melt structure and, therefore, on properties of silicate melts. Several models have been suggested based in part on liquidus phase relations (e.g., Wasserburg, 1957; Burnham, 1975; Nekvasil and Burnham, 1987), in part via theoretical modeling (e. g., Zheng and Nekvasil, 1996; Sykes and Kubicki, 1993, 1994), and in part from spectroscopic studies of quenched melts (glasses) (e.g., Mysen and Virgo, 1986; Kohn et al., 1989, 1992; Holtz et al., 1996; Zotov et al., 1996; Zotov and Keppler, 1998; Oglesby and Stebbins, 2000; Schmidt et al., 2001a,b; Padro et al., 2003). Most of these studies have been restricted to highly polymerized aluminosilicate systems. Even in this restricted composition range, however, considerable disagreement exists as to how H_2O interacts with the aluminosilicate network.

To help resolve the problems associated with solution and solution mechanisms of H_2O in silicate melts, it is necessary to simplify the chemical complexity of the silicate melt. For example, experimental studies in binary metal oxide silicate melts may illuminate how alkali metals and alkaline earths interact with dissolved H_2O and the extent to which H_2O may react with bridging oxygen to form Si-OH groups in the melts and glasses (e.g., Mysen and Virgo, 1986; Kummerlen et al., 1992; Zotov et al., 1996; Zotov and Keppler, 1998). Existing data demonstrate that OH bonding involving alkalis and alkaline earths is possible, but there exist, to the knowledge of the authors, no systematic data on relationships between H_2O solubility and solubility mechanisms, H_2O content and the alkali/silicon ratio of the melts (degree of melt polymerization). Examination of these matters is the objective of the present study.

* Author to whom correspondence should be addressed (mysen@gl.ciw.edu).

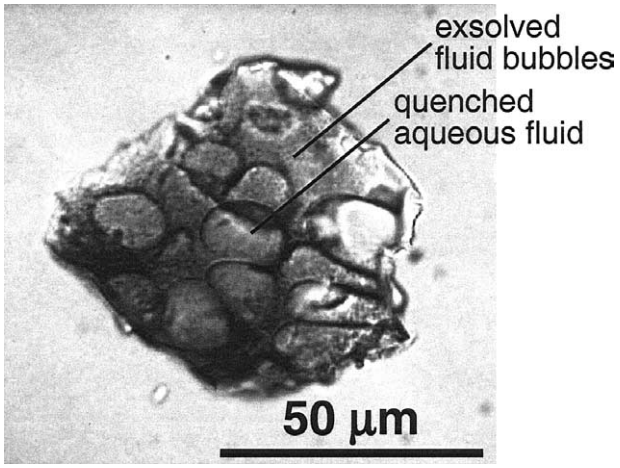

Fig. 1. Electron micrograph of glass chip from run product in the stability field of melt + aqueous fluid with quenched aqueous fluid bubbles and submicron bubbles formed by exsolution during quenching shown. Sample: NS2 + 23 wt% H_2O at 2 GPa and quenched from 1000°C

2. EXPERIMENTAL METHODS

Starting compositions were on the join Na_2O-SiO_2-H_2O. Four compositions were used with nominal NBO/Si of the anhydrous glasses and melts of 0.25, 0.5, 0.75, and 1.0. The samples are denoted NSx, where x represents the number of moles of SiO_2 relative to 1 Na_2O. Anhydrous glasses were made by mixing spectroscopically pure Na_2CO_3, Al_2O_3, and SiO_2, ground under alcohol for ~1 h, decarbonated during slow heating (~1.5°C/min), and then heated at ~100°C above their liquidus temperatures at 0.1 MPa (liquidus data from Osborn and Muan, 1960) for 60 min. The samples were then quenched to glass.

The anhydrous glass starting materials were crushed to ≥20 μm grains size and stored at 250°C when not in use. To ascertain whether or not H_2O from ambient was absorbed in these glasses stored at 250°C, the glasses were subjected to ~1000°C for 60 s to evaluated possible loss on ignition. For glasses more sodic than Na/Si >0.5, this process resulted in ~1 wt% weight loss, which is ascribed to H_2O dissolved in or adsorbed on these glasses. For less sodic glasses, the loss-on-ignition was smaller. In all cases, however, it was assumed that this loss was H_2O. This proportion of H_2O was, therefore, considered part of the total H_2O content of the glasses examined.

High-pressure (0.8–2.0 GPa) and high-temperature (1000°–1300°C) experiments were conducted in the solid-media, high-pressure apparatus (Boyd and England, 1960). The samples were contained in sealed Pt capsules and subjected to experimental pressure and temperature conditions in 0.75-diameter furnace assemblies based on the design of Kushiro (1976). Temperatures were measured with Pt-Pt90Rh10 thermocouples with no correction for pressure on their emf, which may be as much as ± 10°C (Mao et al., 1971). Pressure was calibrated against the melting point of NaCl and the calcite-aragonite transformation (Bohlen, 1984). Estimated uncertainties are ± 10°C and ± 0.1 GPa, respectively.

The starting glasses were loaded together with double-distilled, deionized H_2O (1.0–2.5 μL depending on desired H_2O content) into 3 mm outer diameter (OD) by 7 mm long or 5 mm OD by 10 mm long Pt containers and welded shut. Water was injected using a microsyringe with 0.1 μL divisions. The exact amount of H_2O added was, however, determined by weighing. The weighing accuracy is ± 0.02 mg. Reported H_2O contents of the experimental charges are accurate ± 2% or better [2% for the lowest H_2O contents used (~5 wt% of the total sample)].

Run durations ranged from 300 min at 1300°C to 1440 min at 1000°C. Whether these run durations were sufficient to attain equilibrium can be evaluated by considering the diffusivity of H_2O in the melts. The diffusion constant, D, for H_2O in silicate melts such as those examined here (nominal NBO/Si of anhydrous melts between 0.25 and 1) are likely to be somewhere between those of basaltic and rhyolitic melts at the same temperature and with the same H_2O contents. For those melts, the D-values range between $\sim10^{-8}$ and $\sim10^{-6}$ cm^2/s at temperatures near 1000°C (e.g., Zhang and Stolper, 1991; Nowak and Behrens, 1997). From the simple relationship $x = \sqrt{4Dt}$ (x = diffusion distance, D = diffusion constant, and t = time), even a value for D as low as 10^{-8} cm^2/s would yield a transport distance for H_2O of ~ 270 μm after 300 min. Furthermore, results from time studies of element partitioning between aqueous fluids and hydrous melts using similar sample geometry indicate that ≥800 min are sufficient to reach equilibrium in those experiments (Mysen and Armstrong, 2002). With the ~ 20 μm grain size of the starting material, the ~1440 min run durations are, therefore, more than adequate to ensure equilibrium during the experiments, provided that melt and aqueous fluid remain well mixed during experimentation. This is probably accomplished by convection within the 10 mm long by 3 mm diameter sample containers owing to the ~10°C vertical temperature gradient in the furnaces used (Kushiro, 1976).

Analysis of the quenched glasses for H_2O content by instrumental techniques is difficult because the quenched glasses (quenching rate: ≤100°C/s) in many of these samples contained clouds of finely distributed bubbles (typically <1 μm across) exsolved during quenching (Fig. 1). Similar bubbles were observed in other alkali, and alkaline earth aluminosilicate glasses quenched from similar pressures and temperatures (Mysen and Acton, 1999; Mysen and Wheeler, 2000a; Mysen, 2002) Analysis of the H_2O contents of the glasses by instrumental techniques was unreliable, therefore, because it is not possible to account for H_2O lost by exsolution of H_2O from the melt during temperature quenching of the hydrous melt to a hydrous glass.

To avoid this quenching problem H_2O solubility in the melts was determined by locating the univariant phase boundary, melt ⇔ melt + vapor, by examining the run products in a petrographic microscope (Burnham and Jahns, 1962). This method requires that bubbles in the glass formed by excess H_2O over that needed to saturate the melt at high pressure and temperature, can be distinguished from those formed by H_2O exsolution from the melt during quenching. This distinction is quite straightforward with the hydrous glasses examined in the present study as quench bubbles, when present, form clouds of small, often submicron bubbles. In contrast, bubbles formed by excess H_2O are typically ≥5 μm in diameter (Fig. 1). The uncertainty in the H_2O solubility in melts thus obtained is taken as 1/2 that of each of the melt vs. melt + vapor brackets, and is less than 1 wt%. The reliability of this method was tested by using it to measure the H_2O solubility in $NaAlSi_3O_8$ melt at 1 GPa and 750°C. The observed solubility at these conditions, 17.5 ± 0.5 wt % H_2O, compares well with the 17.2 wt% H_2O at 1 GPa and 690°C reported by Burnham and Jahns (1962).

3. RESULTS AND DISCUSSION

The experimental data are shown in Figures 2–5 where the solid lines represent a third-order polynomial fit of the brackets to temperature at each pressure for each composition. The H_2O solubilities extracted from those data are summarized in Table 1. At 0.8 and 1.3 GPa (Figs. 2 and 3), the pressure-temperature trajectory of the univariant equilibrium, melt ⇔ melt + fluid, could be determined from the experimental charges in the entire 1000°–1300°C temperature of this study from the appearance of large bubbles representing quenched aqueous fluid (Fig. 2). At 1.65 GPa (Fig. 4), the liquidus of NS8+H_2O is somewhere between 1000° and 1100°C because quartz, melt, and fluid coexist at 1000°C at this pressure. Hence, only water solubility data for T ≥1100°C were obtained. At 2.0 GPa (Fig. 5), the melt ⇔ melt + fluid boundary could not be determined for NS8+H_2O because stable fluid bubbles were not detected in experimental charges containing in excess of 40 wt% H_2O. This observation suggests that even at 1000°C and 2.0 GPa, these conditions are above those of the critical curve for this composition (see Paillat et al., 1992, for detailed dis-

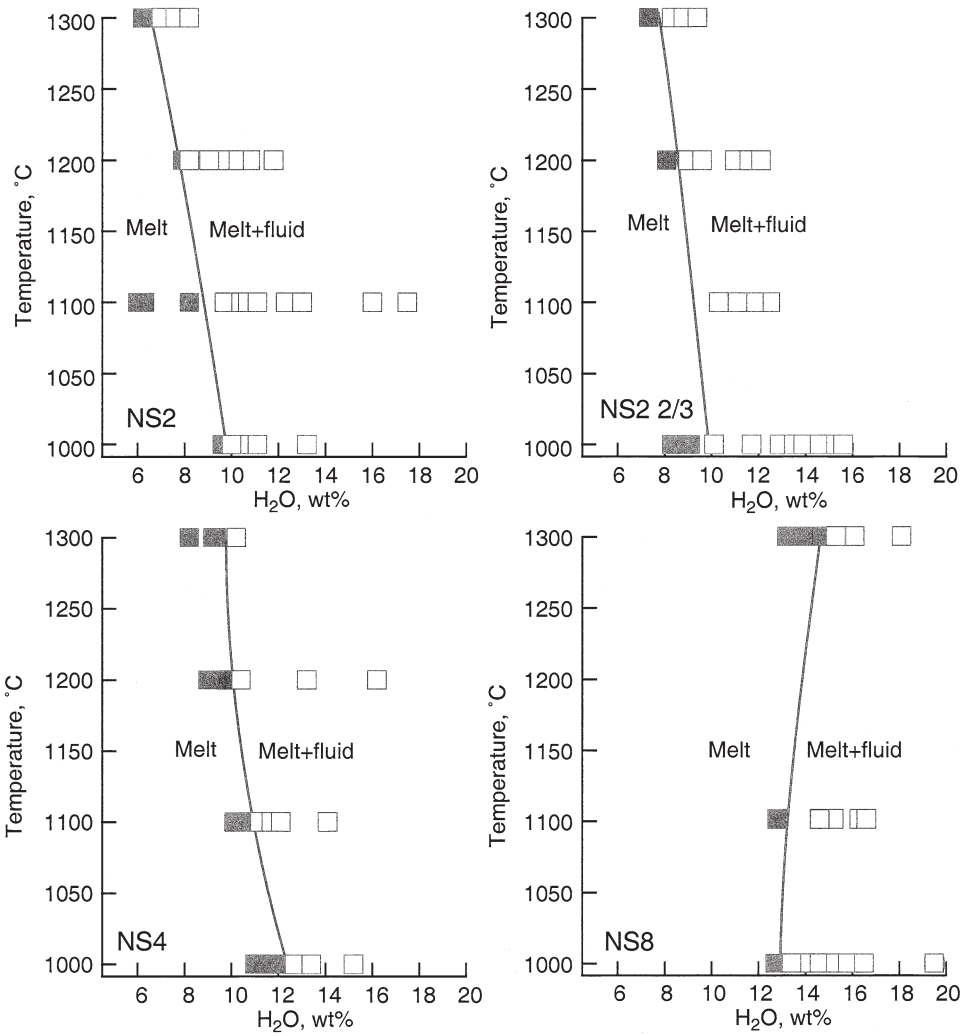

Fig. 2. Experimental results from solubility experiments at 0.8 GPa for compositions NS2, NS2 2/3, NS4, and NS8 as shown on panels. Closed symbols: Hydrous melt only. Open symbols: Hydrous melt + aqueous fluid.

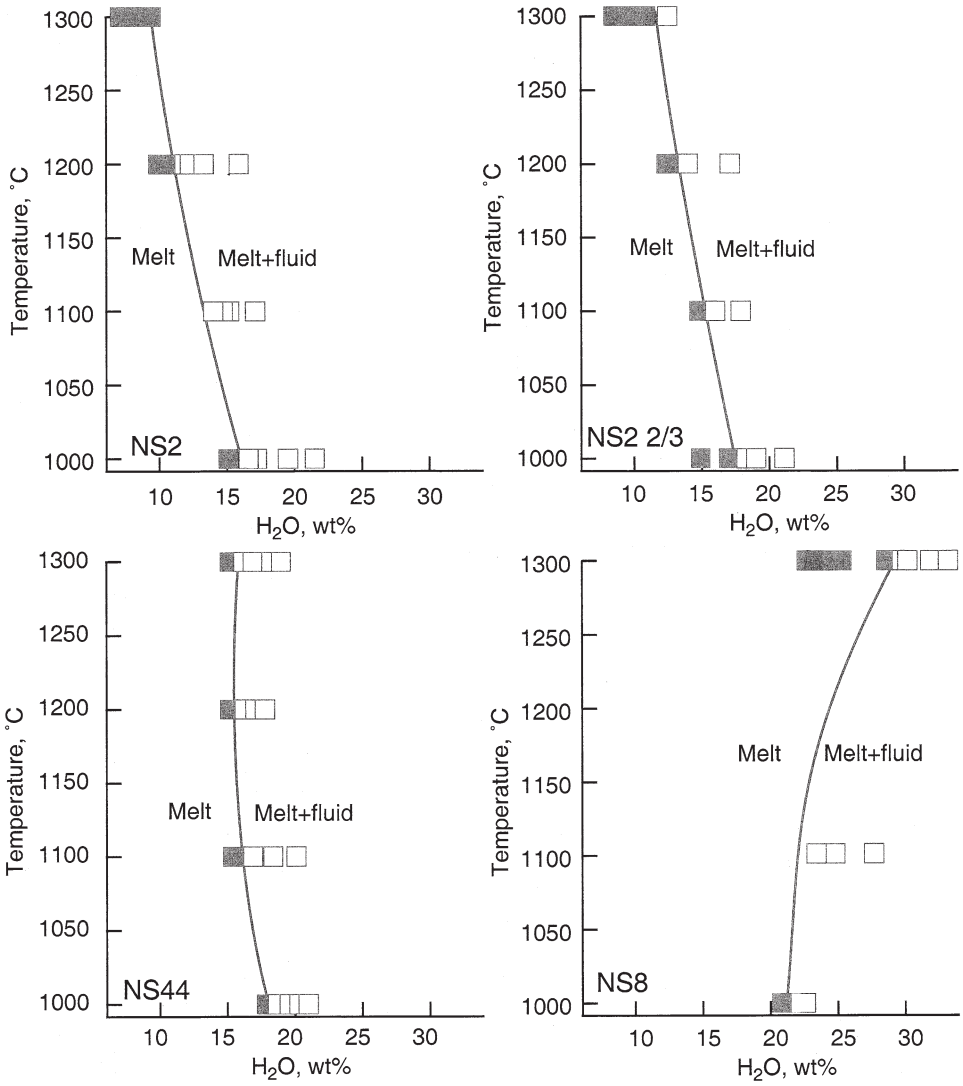

Fig. 3. Experimental results from solubility experiments at 1.3 GPa for compositions NS2, NS2 2/3, NS4, and NS8 as shown on panels. Closed symbols: Hydrous melt only. Open symbols: Hydrous melt + aqueous fluid.

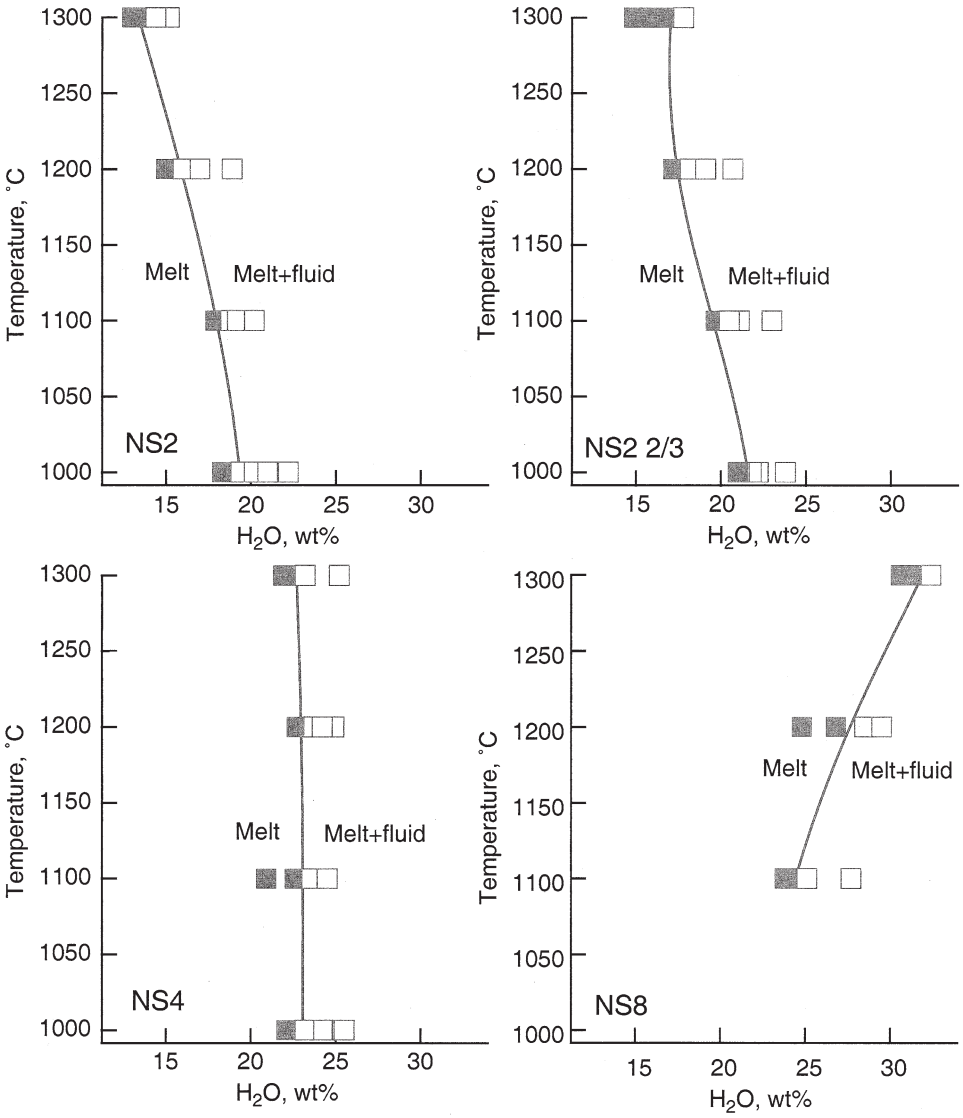

Fig. 4. Experimental results from solubility experiments at 1.65 GPa for compositions NS2, NS2 2/3, NS4, and NS8 as shown on panels. Closed symbols: Hydrous melt only. Open symbols: Hydrous melt + aqueous fluid.

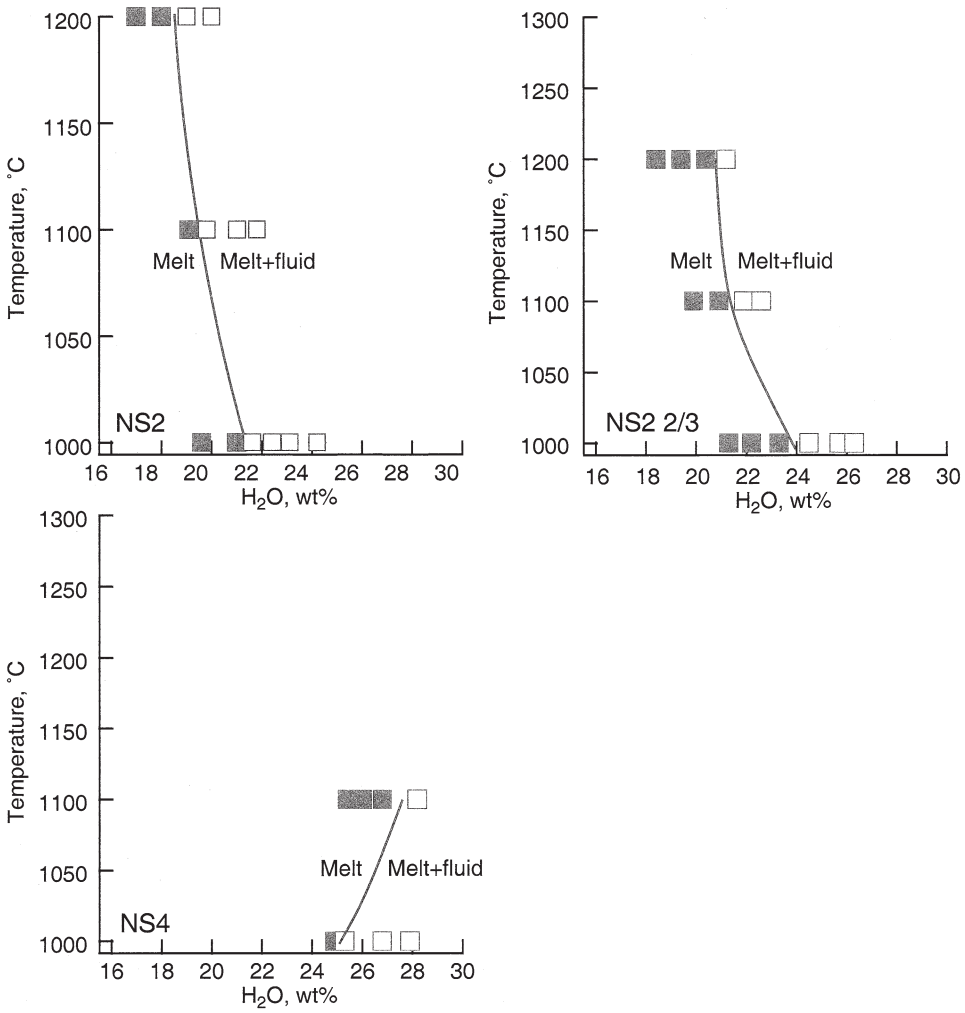

Fig. 5. Experimental results from solubility experiments at 2.0 GPa for compositions NS2, NS2 2/3, NS4, and NS8 as shown on panels. Closed symbols: Hydrous melt only. Open symbols: Hydrous melt + aqueous fluid.

Table 1. Solubility of H_2O as a function of composition, temperature, and pressure.

Composition	Pressure (GPa)	Temperature (°C)	H_2O solubility (mol%, O = 1)
NS2	0.8	10.00	18.5 ± 0.4
NS2	0.8	11.00	16.5 ± 1.0
NS2	0.8	12.00	14.8 ± 0.4
NS2	0.8	13.00	13.0 ± 0.4
NS2	1.3	10.00	26.6 ± 0.7
NS2	1.3	11.00	23.5 ± 0.7
NS2	1.3	12.00	21.3 ± 0.7
NS2	1.3	13.00	19.4 ± 0.6
NS2	1.65	10.00	32.9 ± 0.5
NS2	1.65	11.00	30.0 ± 1.0
NS2	1.65	12.00	27.5 ± 0.9
NS2	1.65	13.00	24.9 ± 0.7
NS2	2	10.00	35.2 ± 0.3
NS2	2	11.00	33.0 ± 0.5
NS2	2	12.00	30.8 ± 0.9
NS2 2/3	−0.8	10.00	18.3 ± 1.1
NS2 2/3	0.8	11.00	17.0 ± 1.1
NS2 2/3	0.8	12.00	15.8 ± 0.7
NS2 2/3	0.8	13.00	14.3 ± 0.7
NS2 2/3	1.3	10.00	29.1 ± 0.8
NS2 2/3	1.3	11.00	26.3 ± 0.7
NS2 2/3	1.3	12.00	23.5 ± 1.4
NS2 2/3	1.3	13.00	21.8 ± 0.7
NS2 2/3	1.65	10.00	35.1 ± 0.7
NS2 2/3	1.65	11.00	32.5 ± 0.7
NS2 2/3	1.65	12.00	30.2 ± 0.8
NS2 2/3	1.65	13.00	28.8 ± 0.8
NS2 2/3	2	10.00	38 ± 1.0
NS2 2/3	2	11.00	34.7 ± 0.8
NS2 2/3	2	12.00	33.9 ± 0.7
NS4	0.8	10.00	19.7 ± 0.3
NS4	0.8	11.00	18.4 ± 0.5
NS4	0.8	12.00	16.5 ± 0.7
NS4	0.8	13.00	16.2 ± 0.7
NS4	1.3	10.00	30.2 ± 0.6
NS4	1.3	11.00	27.5 ± 0.5
NS4	1.3	12.00	26.7 ± 0.8
NS4	1.3	13.00	26.5 ± 0.8
NS4	1.65	10.00	35.4 ± 0.3
NS4	1.65	11.00	35.3 ± 0.8
NS4	1.65	12.00	35.4 ± 0.8
NS4	1.65	13.00	35.7 ± 0.9
NS4	2	10.00	38.5 ± 0.3
NS4	2	11.00	41.4 ± 1.1
NS8	0.8	11.00	20.5 ± 0.7
NS8	0.8	12.00	22.1 ± 1.4
NS8	0.8	13.00	23.4 ± 0.6
NS8	1.3	11	32.0 ± 0.6
NS8	1.3	12	33.9 ± 0.6
NS8	1.3	13	37.5 ± 1.0
NS8	1.65	11	36.3 ± 0.6
NS8	1.65	12	41.2 ± 1.2
NS8	1.65	13	45.9 ± 0.6

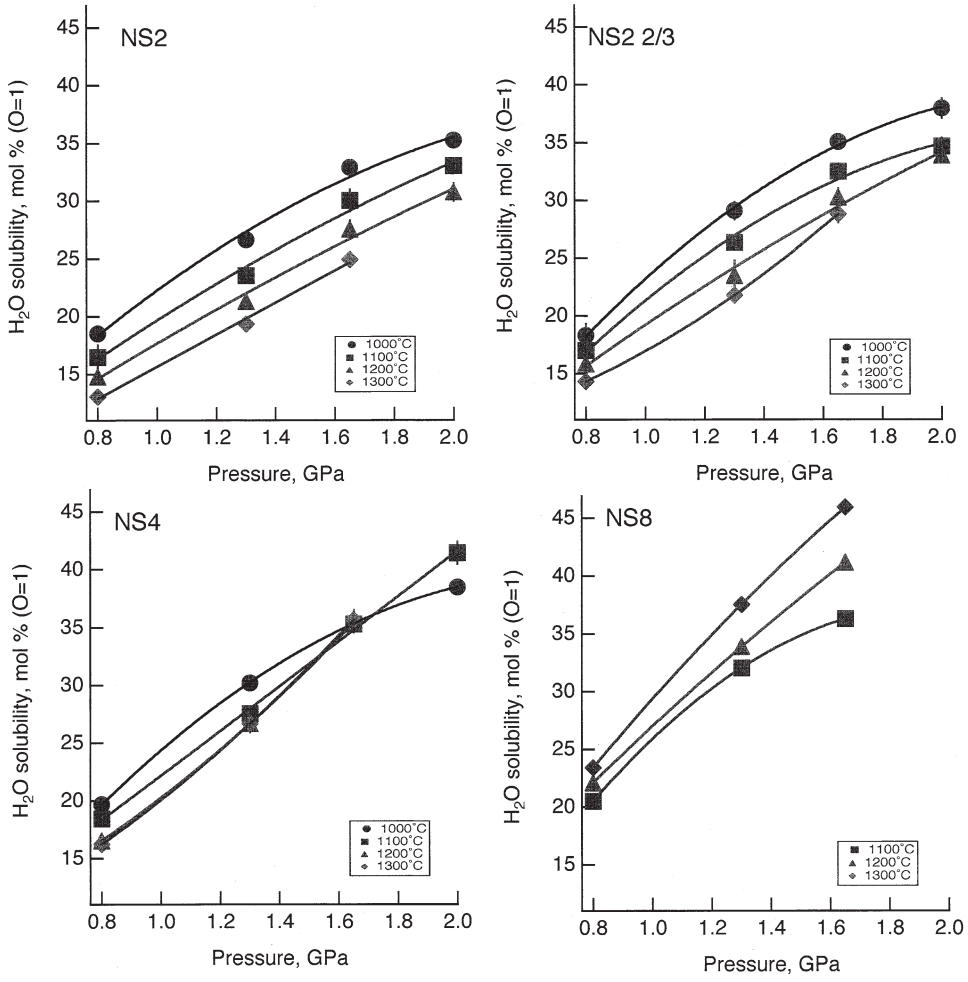

Fig. 6. Solubility of H_2O (in mol % calculated with 1 oxygen in molecular weight) in silicate melt compositions (as shown on individual panels) as a function of pressure for temperature indicated.

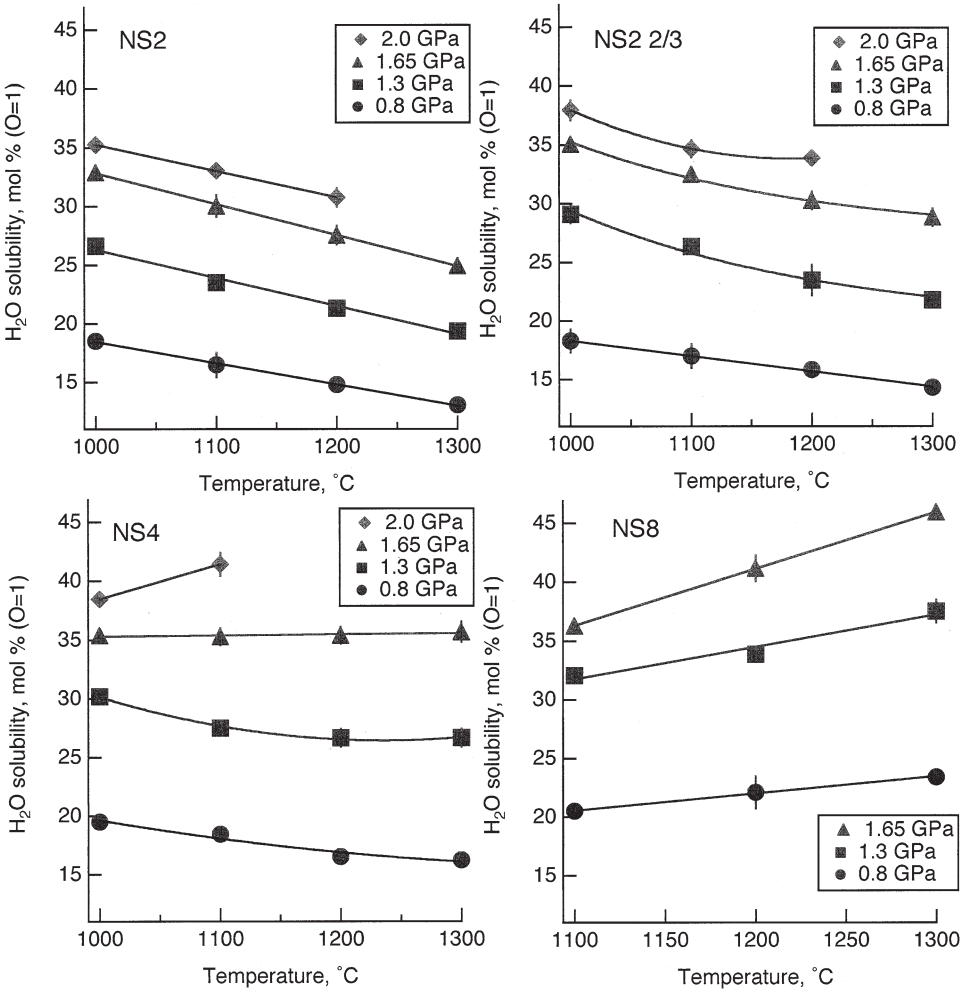

Fig. 7. Solubility of H_2O (in mol % calculated with 1 oxygen in molecular weight) in silicate melt compositions (as shown on individual panels) as a function of temperature for pressures indicated.

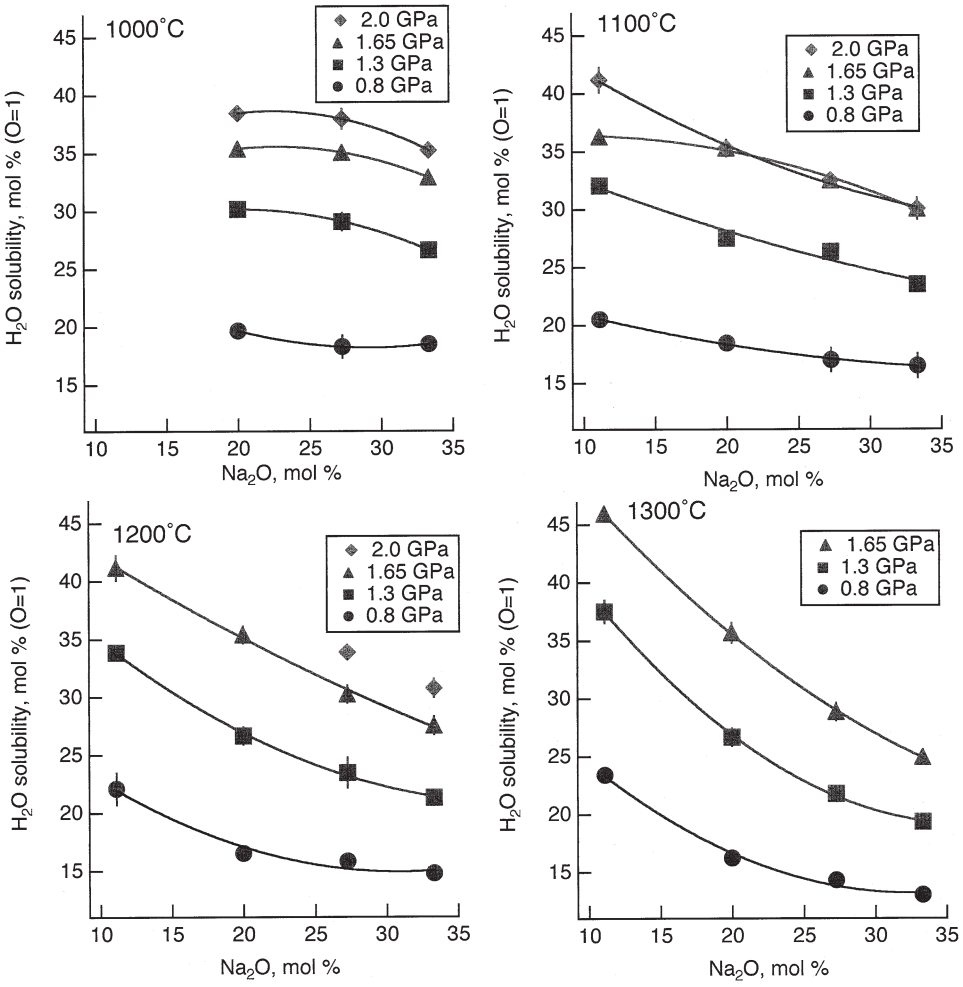

Fig. 8. Solubility of H_2O (in mol % calculated with 1 oxygen in molecular weight) in silicate melt as a function of composition (mol % Na_2O) as a function of pressure and temperature indicated.

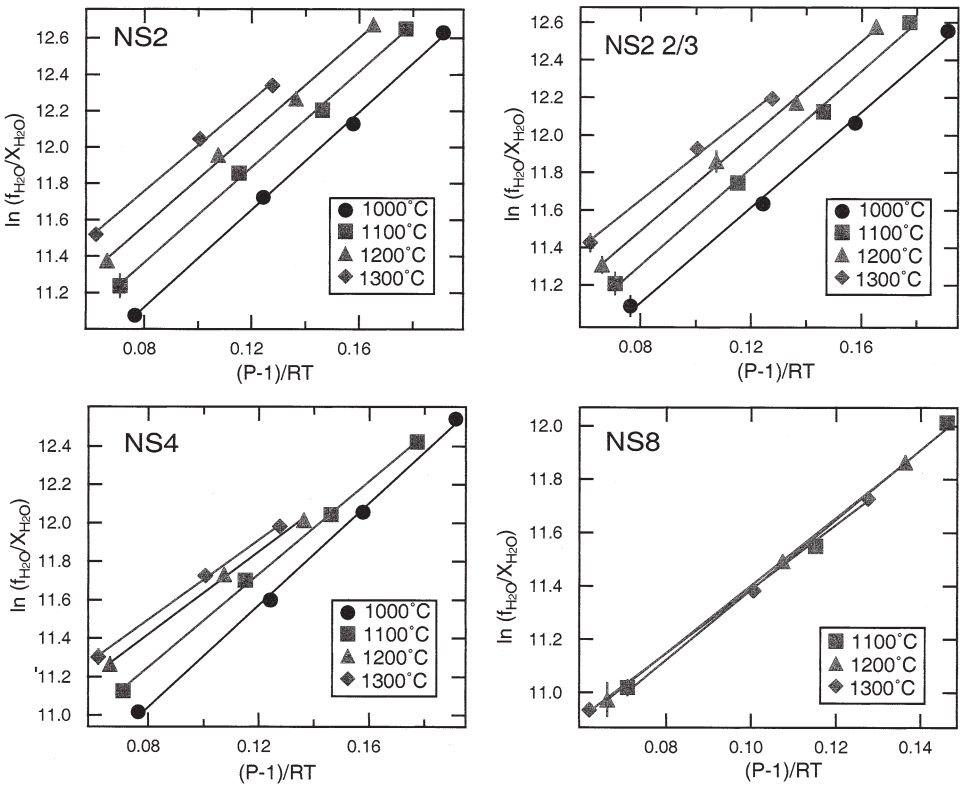

Fig. 9. Relationship between $\ln(f^{o}_{H_2O}/X^{melt}_{H_2O})$ and (P − 1)/RT at temperatures indicated on figures for compositions as indicated on panels at temperatures indicated. When error bars are not shown, errors are smaller than symbol size. See text for more detailed discussion.

cussion of likely P-T trajectories of critical curves in silicate-H_2O systems). In other words, there appears to be complete miscibility between hydrous melts and aqueous fluids for this composition under these pressure and temperature conditions. For NS2 2/3 + H_2O at 2 GPa, this condition occurs at T >1200°C, whereas for NS4 + H_2O fluid and melt could not be distinguished at temperatures above 1100°C. For NS2 + H_2O, there is no evidence from the present experiments suggesting that hydrous melts and aqueous fluids are miscible at the conditions investigated.

Complete miscibility between hydrous melts and silicate-bearing aqueous fluids has been documented via in situ high-temperature and -pressure experiments in the hydrothermal anvil cell. Such data have been reported for systems along the join $NaAlO_2$-SiO_2-H_2O, a haplogranite composition, one peralkaline composition in the $NaAlO_2$-Na_2O-SiO_2-H_2O system as well as for $NaAlSi_3O_8$ with boron and fluorine added (Shen and Keppler, 1997; Bureau and Keppler, 1999; Sowerby and Keppler, 2002). Although there may be some uncertainty in the pressure measurements in these hydrothermal diamond anvil cell experiments (Mysen and Wheeler, 2000b) and the compositions used in those experiments differ from those reported here, the results in Figures 4 and 5 generally are in accord with the results from the hydrothermal diamond anvil cell experiments in that complete miscibility likely occurs at pressures at or above 1 GPa. It is, however, also clear that the exact pressure-temperature coordinates of the critical curves likely depend significantly on silicate composition, consistent with suggestions of Bureau and Keppler (1999).

The results in Table 1 (see also Figs. 2–5) are expressed in terms of pressure, temperature, and composition dependence of H_2O in the melts in Figures 6–8. The isothermal H_2O-solubility (Fig. 6) is positively correlated with pressure, a feature common to all existing H_2O solubility data in silicate melts (see, for example, McMillan, 1994, for review and more recent data by, for example, Dixon and Stolper, 1995; Holtz et al., 1995, 2000; Dingwell et al., 1997; Schmidt et al., 1999; Tamic et al., 2001).

The temperature dependence of H_2O-solubility, $(\partial X_{H2O}/\partial T)_P$, depends on melt composition and pressure (Fig. 7). For the 2 most sodic compositions, NS2 and NS2 2/3, the $(\partial X_{H2O}/\partial T)_P$ becomes decreasingly negative with increasing pressure. For composition NS4, $(\partial X_{H2O}/\partial T)_P$ changes from negative to positive at pressures between 1.3 and 2.0 GPa with $(\partial X_{H2O}/\partial T)_P \sim 0$ at 1.65 GPa. The $(\partial X_{H2O}/\partial T)_P$ for the most silica-rich composition Na_2O-SiO_2 composition, NS8, is positive at all pressures studied. No other data exist for comparable compositions in the pressure/temperature range of the present experiments. However, at lower pressures (near 0.5 GPa), the $(\partial X_{H2O}/\partial T)_P$ of highly polymerized compositions such as $NaAlSi_3O_8$ and haplogranite (an albite-orthoclase-quartz mixture; see, for example, Holtz et al., 2000), changes from negative to positive (Paillat et al., 1992; Holtz et al., 2000). Thus, the present data are generally consistent with those observa-

tions that increasing pressure leads to change from decreasing to increasing H_2O-solubility with increasing temperature. The solubility data are also consistent with the general concept that with increasing pressure the melt-fluid immiscibility gap shrinks and the critical temperature decreases (e.g., Paillat et al., 1992; Bureau and Keppler, 1999).

Under isothermal and isobaric conditions, the H_2O-solubility in Na_2O-SiO_2-H_2O melts decreases with increasing Na_2O content (Fig. 8). This relationship is more pronounced the higher the temperature and the higher the pressure. To our knowledge, there exist not data with which to compare these results in the pressure and temperature range of the present experiments. The relationships in Figure 8 do suggest that the solution mechanism of H_2O in these melts may depend on silicate composition (see also further discussion below). Otherwise, silicate composition-dependent H_2O might be difficult to rationalize.

The H_2O solubility data presented in Figures 2–4 and Table 1 can be used to estimate partial molar volumes of H_2O in the melts. For H_2O-saturated melt in equilibrium with free H_2O, the Gibbs free energy of solution of H_2O is (J/mol);

$$\Delta G_T(P) = 0 = \Delta G_T(1\ bar) + RT \ln \frac{a^{melt}_{H_2O}}{f^{o}_{H_2O}} + \int_1^P \bar{V}^{melt}_{H_2O} dP, \quad (1)$$

where R is the universal gas constant (82.157 cm^3bar/mol K), T is temperature (Kelvin), $a^{melt}_{H_2O}$ is activity of H_2O in the melt, $f^{o}_{H_2O}$ is the fugacity of pure H_2O in bar, and $\bar{V}^{melt}_{H_2O}$ (cm^3/mol) is the partial molar volume of H_2O in the melt. The activity of H_2O, $a^{melt}_{H_2O}$, is not known. We assume, therefore, that the mol fraction, $x^{melt}_{H_2O}$, may be substituted for $a^{melt}_{H_2O}$. Calorimetric data for $NaAlSi_3O_8$-H_2O glasses indicate only a small negative heat of mixing (0–49 kJ/mol) (Clemens and Navrotsky, 1987). The assumption $a^{melt}_{H2O} = X^{melt}_{H2O}$ would not, therefore, introduce a large error in calculations of $\bar{V}^{melt}_{H_2O}$ from solubility.

The slope of the (P − 1)/RT vs. $\ln\left(\int^{o}_{H_2O}/X^{melt}_{H_2O}\right)$ equals $\bar{V}^{melt}_{H_2O}$ at given temperature, T (e.g., Lange, 1994). In the 0.8–2.0 GPa pressure range examined here, these lines are straight (Fig. 9). The uncertainty in $\bar{V}^{melt}_{H_2O}$ reflects the progression of the errors in the measured water solubilities for the melts. These straight lines are consistent with a suggestion that the partial molar volume of H_2O, $\bar{V}^{melt}_{H_2O}$, does not vary with pressure in the 0.8–2.0 GPa pressure range within the uncertainty of the calculated partial molar volume values for melts saturated with H_2O at the pressures used.

The $\bar{V}^{melt}_{H_2O}$ derived from the slopes in Figure 9 ranges between ~10 and 14 cm^3/mol with a slight negative temperature dependence (Fig. 10A). The $\bar{V}^{melt}_{H_2O}$ also depends slightly on silicate composition with minimum $\bar{V}^{melt}_{H_2O}$-values for compositions with ~20 mol % Na_2O (Fig. 10B). A comparison of $\bar{V}^{melt}_{H_2O}$ in NS4 melt with $\bar{V}^{melt}_{H_2O}$ for melts with the same nominal NBO/Si-value but different metal oxide (K_2O and CaO; see Mysen and Acton, 1999; Mysen, 2002; see open symbols in Fig. 10A) suggests that $\bar{V}^{melt}_{H_2O}$ may be positively correlated with the ionization potential of the metal cation.

The $\bar{V}^{melt}_{H_2O}$ values in Figure 10 (>10 to ~ 14 cm^3/mol) compare reasonably well with those calculated from water solubility data for haplogranite ($Qz_{28}Ab_{38}Or_{34}$), albite, and diopside composition melts (Hodges, 1974; Paillat et al., 1992; Holtz et al., 1995), and for a composition in the CaO-Al_2O_3-SiO_2-H_2O system by McMillan et al. (1986) [NBO/T = 0.6, Al/(Al + Si)+0.14]. Those values (~11 to ~18 cm^3/mol) also are in the same range as the values reported from direct measurements of $\bar{V}^{melt}_{H_2O}$ for andesite glass and SiO_2 (Richet and Polian, 1998; Richet et al., 2000) and $NaAlSi_3O_8$ melt (Burnham and Davis, 1971; Kushiro, 1978; Ochs and Lange, 1997).

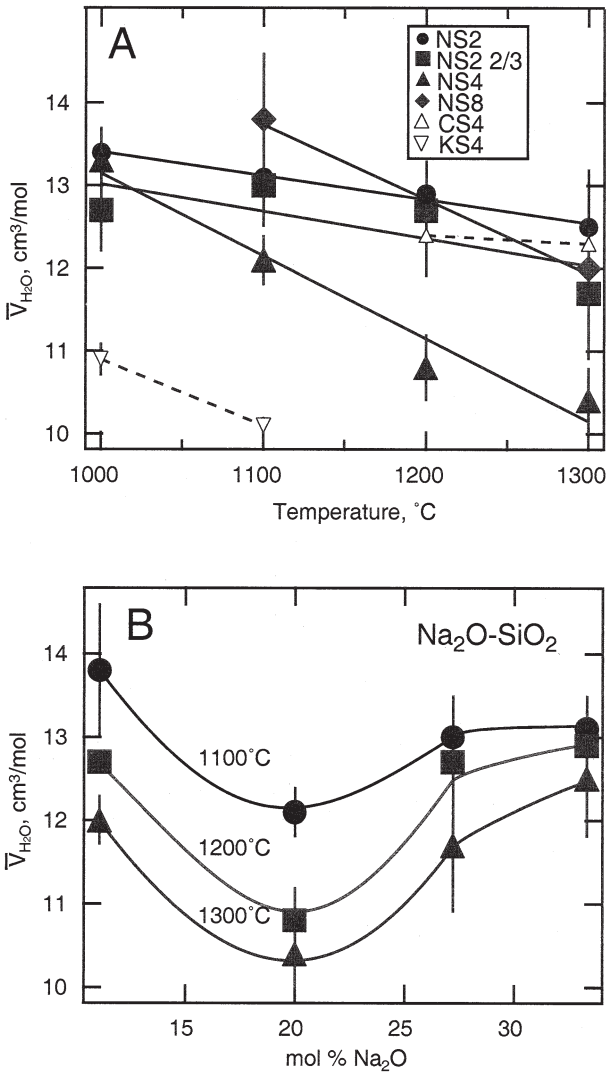

Fig. 10. Partial molar volume of H_2O in melts, $\bar{V}^{melt}_{H_2O}$ A. as a function of temperature for compositions indicated (CS4 and KS4 are compositions $CaSi_4O_9$ and $K_2Si_4O_9$, respectively. Those data are from Mysen, 2002, and Mysen and Acton, 1999), and B. for melt composition for temperatures indicated. These $\bar{V}^{melt}_{H_2O}$ values were calculated with Eqn. 1 for H_2O-saturated melts in the 0.8–2.0 GPa pressure range.

Acknowledgments—This research was conducted with partial support from NSF grants EAR-9901886, 0405383, and an REU grant from NSF to the Carnegie Institution of Washington.

Associate editor: F. J. Ryerson

REFERENCES

Behrens H., Meyer M., Holtz F., and Nowak M. (2001) The effect of alkali ionic radius, temperature and pressure on the solubility of water in $MAlSi_3O_8$ melts (M = Li, Na, K, Rb). *Chem. Geol.* **174,** 275–289.

Bohlen S. R. (1984) Equilibria for precise pressure calibration and a frictionless furnace assembly for the piston-cylinder apparatus. *N. Jb. Mineral., Mh.* **84**(*9*), 404–412.

Boyd F. R. and England J. L. (1960) Apparatus for phase equilibrium measurements at pressures up to 50 kilobars and temperatures up to 1750°C. *J. Geophys. Res.* **65,** 741–748.

Bureau H. and Keppler H. (1999) Complete miscibility between silicate melts and hydrous fluids in the upper mantle; experimental evidence and geochemical implications. *Earth Planet. Sci. Lett.* **165** (*2*), 187–196.

Burnham C. W. (1975) Water and magmas: A mixing model. *Geochim. Cosmochim. Acta* **39** (*8*), 1077–1084.

Burnham C. W. and Jahns R. H. (1962) A method for determining the solubility of water in silicate melts. *Am. J. Science* **260,** 721–745.

Burnham C. W. and Davis N. F. (1971) The role of H_2O in silicate melts. I. P-V-T relations in the system $NaAlSi_3O_8$-H_2O to 10 kilobars and 1000C. *Am. J. Sci.* **270,** 54–79.

Carroll M. R. and Blank J. G. (1997) The solubility of H_2O in phonolitic melts. *Am. Mineral.* **82** (*5–6*), 549–556.

Clemens J. D. and Navrotsky A. (1987) Mixing properties of $NaAlSi_3O_8$-H_2O melts; new calorimetric data and some geological implications. *J. Geol.* **95,** 173–186.

Dingwell D. B., Holtz F., and Behrens H. (1997) The solubility of H_2O in peralkaline and peraluminous granitic melts. *Am. Mineral.* **82,** 434–437.

Dingwell D. B., Hess K.-U., and Romano C. (1998) Viscosity data for hydrous peraluminous granitic melts: Comparison with the metaluminous model. *Am. Mineral.* **83,** 236–239.

Dixon J. E. and Stolper E. M. (1995) An experimental study of water and carbon dioxide solubilities in mid-ocean ridge basaltic liquids—Part II. Applications to degassing. *J. Petrol.* **36** (*6*), 1633–1646.

Gaetani G. A., Grove T. L., and Bryan W. B. (1993) The influence of water on the petrogenesis of subduction-related igneous rocks. *Nature* **365,** 332–334.

Goranson R. W. (1936) Silicate-water systems: The solubility of water in albite-melt. *Trans. Am. Geophys. Union* **17,** 257–259.

Hamilton D. L., Burnham C. W., and Osborn E. F. (1964) The solubility of water and the effects of oxygen fugacity and water content on crystallization of mafic magmas. *J. Petrol.* **5,** 21–39.

Hamilton D. L. and Oxtoby S. (1986) Solubility of water in albite melt determined by the weight loss method. *J. Geol.* **94,** 616–630.

Hodges F. N. (1974) The solubility of H_2O in silicate melts. *Carnegie Instn. Wash. Year Book* **73,** 251–255.

Holtz F., Behrens H., Dingwell D. B., and Johannes W. (1995) H_2O solubility in haplogranitic melts: Compositional, pressure and temperature dependence. *Am. Mineral.* **80,** 94–108.

Holtz F., Scaillet B., Behrens H., Schulze F., and Pichavant M. (1996) Water contents of felsic melts; application to the rheological properties of granitic magmas. In *The Third Hutton Symposium on the Origin of Granites and Related Rocks*, Vol. 315 (eds. M. Brown, P. A. Candela, D. L. Peck, W. E. Stephens, R. J. Walker, and E. A. Zen), pp. 57–64. Geological Society of America.

Holtz F., Roux J., Ohlhorst S., Behrens H., and Schulze F. (1999) The effects of silica and water on the viscosity of hydrous quartzofeldspathic melts. *Am. Mineral.* **84,** 27–36.

Holtz F., Roux J., Behrens H., and Pichavant M. (2000) Water solubility in silica and quartzofeldspathic melts. *Am. Mineral.* **85,** 682–686.

Kohn S. C., Dupree R., and Smith M. E. (1989) A multinuclear magnetic resonance study of the structure of hydrous albite glasses. *Geochim. Cosmochim. Acta* **53** (*11*), 2925–2935.

Kohn S. C., Dupree R., and Mortuza M. G. (1992) The interaction between water and aluminosilicate magma. *Chem. Geol.* **96,** 399–410.

Kummerlen J., Merwin L. H., Sebald A., and Keppler H. (1992) Structural role of H_2O in sodium silicate glasses: Results from ^{29}Si and ^{1}H NMR spectroscopy. *J. Phys. Chem.* **96,** 64–5; 6410.

Kushiro I. (1972) Effect of water on the composition of magmas formed at high pressures. *J. Petrol.* **13,** 311–334.

Kushiro I. (1976) A new furnace assembly with a small temperature gradient in solid-media, high-pressure apparatus. *Carnegie Inst. Wash. Year Book* **75,** 832–833.

Kushiro I. (1978) Viscosity and structural changes of albite ($NaAlSi_3O_8$) melt at high pressures. *Earth Planet. Sci. Lett.* **41,** 87–91.

Kushiro I. (1990) Partial melting of mantle wedge and evolution of island arc crust. *J. Geophys. Res.* **95,** 15929–15939.

Lange R. A. (1994) The effect of H_2O, CO_2 and F on the density and viscosity of silicate melts. In *Volatiles in Magmas* (eds. M. R. Carroll and J. R. Holloway), pp. 331–370. Mineralogical Society of America.

Mao H. K., Bell P. M., and England J. L. (1971) Tensional errors and drift of the thermocouple electromotive force in the single stage, Piston-cylinder apparatus. *Carnegie Inst. Wash. Year Book* **70,** 281–287.

McMillan P., Peraudeau G., Holloway J. R., and Coutoures J.-P. (1986) Water solubility in calcium aluminosilicate melt. *Contr. Mineral. Petrol.* **94,** 178–182.

McMillan P. F. (1994) Water solubility and speciation models. In *Volatiles in Magmas*, Vol. 30 (ed. M. R. Carroll and J. R. Holloway), pp. 131–156. Mineralogical society of America.

Mysen B. O. (1992) Peralkalinity, Al,Si substitution and solubility mechanisms of H_2O in aluminosilicate melts. *J. Petrol.* **33,** 347–375.

Mysen B. O. (2002) Solubility of alkaline earth and alkali aluminosilicate components in aqueous fluids in the Earth's upper mantle. *Geochim. Cosmochim. Acta* **66,,** 2421–2438.

Mysen B. O. and Boettcher A. L. (1975) Melting of a hydrous mantle. II. Geochemistry of crystals and liquids formed by anatexis of mantle peridotite at high pressures and high temperatures as a function of controlled activities of water, hydrogen and carbon dioxide. *J Petrol.* **16,** 549–590.

Mysen B. O. and Virgo D. (1986) The structure of melts in the system Na_2O-CaO-Al_2O_3-SiO_2-H_2O quenched from high temperature at high pressure. *Chem. Geol.* **57,,** 333–358.

Mysen B. O. and Acton M. (1999) Water in H_2O-saturated magma-fluid systems: Solubility behavior in K_2O-Al_2O_3-SiO_2-H_2O to 2.0 GPa and 1300°C. *Geochim. Cosmochim. Acta* **63,** 3799–3816.

Mysen B. O. and Wheeler K. (2000a) Solubility behavior of water in haploandesitic melts at high pressure and high temperature. *Am. Mineral.* **85,** 1128–1142.

Mysen B. O. and Wheeler K. (2000b) Alkali aluminosilicate-saturated aqueous fluids in the Earth's upper mantle. *Geochim. Cosmochim. Acta* **64,** 4243–4256.

Mysen B. O. and Armstrong L. (2002) Solubility behavior of alkali aluminosilicate components in aqueous fluids and silicate melts at high pressure and temperature. *Geochim. Cosmochim. Acta* **66,** 2287–2298.

Nekvasil H. and Burnham C. W. (1987) The calculated individual effects of pressure and water content on phase equilibria in the granite system. In *Magmatic Processes: Physicochemical Principles* (ed. B. O. Mysen), pp. 433–446. Geochemical Society of America.

Nowak M. and Behrens H. (1995) The speciation of water in haplogranitic glasses and melts by in-situ, near-infrared spectroscopy. *Geochim. Cosmochim. Acta* **59,** 3445–3450.

Nowak M. and Behrens H. (1997) An experimental investigation on diffusion of water in haplogranitic melts. *Contrib. Mineral. Petrol.* **126,** 365–376.

Ochs F. A. and Lange R. A. (1997) The partial molar volume, thermal expansivity and compressibility of H_2O in $NaAlSi_3O_8$ liquid: New measurements and an internally consistent model. *Contrib. Mineral. Petrol.* **129,** 155–165.

Oglesby J. V. and Stebbins J. F. (2000) ^{29}Si CPMAS NMR investigations of silanol-group minerals and hydrous aluminosilicate glasses. *Am. Mineral.* **85,** 722–731.

Osborn E. F. and Muan A. (1960) Phase equilibrium diagrams for ceramists. Plate 4. The system Na_2O-Al_2O_3-SiO_2. American Ceramic Society.

Padro D., Schmidt B. C., and Dupree R. (2003) Water solubility mechanism in hydrous aluminosilicate glass: Information from 27A1 MAS and MQMAS NMR. *Gechim. Cosmochim. Acta* **67,** 1543–1552.

Paillat O., Elphick E. C., and Brown W. L. (1992) The solubility behavior of H_2O in $NaAlSi_3O_8$ melts: A re-examination of Ab-H_2O phase relationships and critical behavior at high pressure. *Contrib. Mineral. Petrol.* **112,** 490–500.

Richet P. and Polian A. (1998) Water as a dense icelike component in silicate glasses. *Science* **281** (*5375*), 396–398.

Richet P., Whittington A., Holtz F., Behrens H., Ohlhorst S., and Wilke M. (2000) Water and the density of silicate glasses. *Contrib. Mineral. Petrol.* **138,** 337–347.

Romano C., Poe B. T., Mincione V., Hess K. U., and Dingwell D. B. (2001) The viscosities of dry and hydrous $XAlSi_3O_8$ (X = Li, Na, K, $Ca_{0.5}$, $Mg_{0.5}$) melts. *Chem. Geol.* **174,,** 115–132.

Schmidt B., Holtz F., and Pichavant M. (1999) Water solubility in haplogranitic melts coexisting with H_2O-H_2 fluids. *Contrib. Mineral. Petrol.* **136,** 213–224.

Schmidt B. C., Behrens H., Riemer T., Kappes R., and Dupree R. (2001a) Quantitative determination of water speciation in aluminosilicate glasses: A comparative NMR and IR spectroscopic study. *Chem. Geol.* **174,** 195–208.

Schmidt B. C., Riemer T., Kohn S. C., Holtz F., and Dupree R. (2001b) Structural implications of water dissolution in haplogranitic glasses from NMR spectroscopy: Influence of total water content and mixed alkali effect. *Geochim. Cosmochim. Acta* **65,** 2949–2964.

Schulze F., Behrens H., Holtz F., Roux J., and Johannes W. (1996) The influence of H_2O on the viscosity of haplogranitic melt. *Am. Mineral.* **81,** 1155–1165.

Shen A. and Keppler H. (1995) Infrared spectroscopy of hydrous silicate melts to 1000°C and 10 kbar: Direct observation of H_2O speciation in a diamond cell. *Am. Mineral.* **80,** 1335–1338.

Shen A. H. and Keppler H. (1997) Direct observation of complete miscibility in the albite-H_2O system. *Nature* **385,** 710–712.

Silver L. and Stolper E. (1985) A thermodynamic model for hydrous silicate melts. *J. Geol.* **93,** 161–178.

Silver L. and Stolper E. (1989) Water in albitic glasses. *J. Petrol.* **30,** 667–710.

Sowerby J. R. and Keppler H. (1999) Water speciation in rhyolitic melt determined by in-situ infrared spectroscopy. *Am. Mineral.* **84,** 1843–1849.

Sowerby J. R. and Keppler H. (2002) The effect of fluorine, boron and excess sodium on the critical curve in the albite-H_2O system. *Contrib. Mineral. Petrol.* **143,** 32–37.

Stolper E. (1982) Water in silicate glasses: An infrared spectroscopic study. *Contr. Mineral. Petrol.* **81,** 1–17.

Sykes D. and Kubicki J. D. (1993) A model for H_2O solubility mechanisms in albite melts from infrared spectroscopy and molecular orbital calculations. *Geochim. Cosmochim. Acta* **57,** 1039–1052.

Tamic N., Behrens H., and Holtz F. (2001) The solubility of H_2O and CO_2 in rhyolitic melts in equilibrium with a mixed CO_2-H_2O fluid phase. *Chem. Geol.* **174,** 333–347.

Wasserburg G. J. (1957) The effects of H_2O in silicate systems. *J. Geol.* **65,** 15–23.

Watson E. B. (1994) Diffusion in volatile-bearing magmas. In *Volatiles in Magmas*, Vol. 30 (eds. M. R. Carroll and J. R. Holloway), pp. 371–411. Mineralogical Society of America.

Withers A. C., Zhang Y., and Behrens H. (1999) Reconciliation of experimental results on H_2O speciation in rhyolitic glass using in-situ and quenching techniques. *Earth Planet. Sci. Lett.* **173,** 343–349.

Zhang Y. (1999) H_2O in rhyolitic glasses and melts: Measurements, speciation, solubility and diffusion. *Rev. Geophys.* **37,** 493–516.

Zhang Y. and Stolper E. M. (1991) Water diffusion in a basaltic melt. *Nature* **351** (*6324*), 306–309.

Zhang Y., Stolper E. M., and Ihinger P. D. (1995) Kinetics of the reaction $H_2O+O=2OH$ in rhyolitic and albitic glasses: Preliminary results. *Amer. Mineral.* **80,** 593–612.

Zheng Q. and Nekvasil H. (1996) An associated solution model for albite-water melts. *Geochim. Cosmochim. Acta* **60,** 59–74.

Zotov N., Keppler H., Hannon A. C., and Soper A. K. (1996) The effect of water on the structure of silicate glasses—A neutron diffraction study. *J. Non-Cryst. Solids* **202,** 153–163.

Zotov N. and Keppler H. (1998) The influence of water on the structure of hydrous sodium tetrasilicate glasses. *Am. Mineral.* **83,** 823–834.